Full Length Article

# Moderate noise associated oxidative stress with concomitant memory impairment, neuro-inflammation and neurodegeneration

Manish Shukla [a], Kumar Vyonkesh Mani [a], Deepshikha [a], Sangeeta Shukla [b], Neeru Kapoor [a,*]

[a] Occupational Health Division, Defence Institute of Physiology & Allied Sciences (DIPAS), DRDO Lucknow Road, Timarpur, Delhi, India
[b] School of Studies in Zoology, Jiwaji University, Gwalior, M.P., India

A B S T R A C T

Noise, a disturbing and unwanted sound is currently being perceived as a widespread environmental stressor. In the present study we investigated the activation of oxidative stress as a mechanism involved in cognitive impairment through changes in neuro-inflammation.

Sprague Dawley rats (200-220 g m) were exposed to moderate (100dB) sound pressure level (SPL) noise daily for 2 h s over a period of 15 and 30 days and the consequence on brain regions of hippocampus observed through behavioral studies by Morris Water Maze to assess effects on spatial memory coupled with biochemical evaluation of markers of oxidative stress and inflammation. Further, the underlying mechanism pertaining to apoptosis was investigated by immuno-histological studies through assessment of Caspase-3 and TUNEL assay as well as morphological parameters, namely Nissl bodies in CA1, CA3 and DG regions of hippocampus.

Poorer performance in the MWM indicative of decrement in concept formation, attention, working memory, and reference memory was observed on 15 and 30 days of noise exposures. At the cellular level, increased oxidative stress and inflammation was noticed as evinced by elevated levels of TNF-α, IL-6, IL-1α and IFN-γ in both hippocampus and plasma. Exposure to noise also led to a gradual increase in the number of pyknotic and apoptotic neurons together with the increase in DNA fragmentation in hippocampus. Increased levels of inflammatory genes (i.g.) *ccl2, ccr5, ifng, il13, il1a, tnfa* coupled with decreased levels of *bmp2* and *il3* genes were found in both the noise exposure groups.

Our findings revealed that moderate intensity noise exposure impaired early memory changes in expression of several gene families including genes associated with regulation of transcription, inflammatory response, and, response to oxidative stress.

## 1. Introduction

Noise, a disturbing and unwanted sound is currently being perceived as a widespread environmental stressor. The response to noise depends on characteristics of the sound including intensity and frequency, its complexity, duration and the meaning it conveys. Exposure to noise is detrimental to hearing and impairs health by disturbing the sleep, affecting cognition leading to psycho physiological and behavioral changes with decrement in performance (Cui et al., 2012).

As early as 1984, Daniel reported that noise exposures exceeding 90dB constituted a source of stress (Daniel, 1984). Previous reports have established that rats exposed continuously to noise levels at 100dB/4hr per day for 30 days exhibit significant increase in the working and reference memory errors when compared to control animals. Spatial learning and memory are coordinated by different brain regions, particularly hippocampus. A study carried out on rat model showed that acute as well as long term exposure to noise can produce excessive free radicals (ROS), disrupting normal cellular functions and integrity (Manikandan et al., 2006). The formation of ROS occurs when unpaired electrons escape the electron transport chain and react with molecular oxygen, generating superoxide. Superoxide can react with DNA, proteins, and lipids and plays an important role in many physiological and pathophysiological conditions, notably ischemia-reperfusion injury, neurodegenerative diseases, and aging (Balaban et al., 2005). ROS can also react with nitric oxide (NO), generating reactive nitrogen species (RNS) (Brown and Borutaite, 2001).

---

Cytokines are known to play a crucial role in inflammation, neuro-behavioral and emotional deficits. During the inflammatory challenge, microglial cells get activated and affect the release of cytokines (pro-inflammatory cytokines increase and anti-inflammatory cytokines decrease), often coinciding with behavioral manifestations(Kang et al., 2014; Wohleb et al., 2014). ROS can also lead to inflammation, including the production of pro inflammatory cytokines such as IL-6 (Wakabayashi et al., 2010), TNF-α (Keithley et al., 2008), that serve as mediators triggering cell death (Tan et al., 2016) via activation of NF-kB signaling cascade leading to production of cytokines. The expression of many pro-inflammatory mediators that participate in the acute inflammatory response is broadly regulated by the transcription factor NF-kB (Denk et al., 2000).

Despite these findings, the mechanism underlying noise induced hearing loss (NIHL) is not explicit. The present study aimed to determine the consequences of noise stress on memory impairment and explore its underlying mechanism. We ascertained the noise exposure duration associated with maximum changes in spatial memory and consolidation, examined the effect of retraining on memory consolidation affected during noise, and, studied the neuronal morphology, apoptosis and DNA fragmentation in an attempt to analyze the role of neurodegeneration as a possible underlying mechanism. This study revealed the expression of several gene families including genes associated with regulation of transcription, inflammatory response, and response to oxidative stress. For a more elaborate quantification and characterization of the roles of inflammatory and cytokines receptor in noise-induced memory impairment, a panel of 84 inflammatory and cytokines receptor-related genes was screened using quantitative real-time PCR array, a method that features a high degree of sensitivity, selectivity and accuracy.

## 2. Material and methods

### 2.1. Experimental animals and experiment design

Male Sprague-Dawley rats (200–220 g) were placed in pairs in Plexiglas cages in the institutional animal house, maintained at standard environmental conditions of temperature ($25 \pm 2$ °C) and humidity ($55 \pm 2\%$ RH). Food pellets (Lipton Pvt. Limited) and water *at libitum* was provided to the animals. The experiments were performed in consistence with the guidelines of Institutional Animal Ethics Committee. Efforts were made to minimize the number of animals within statistical limits and pain to the animals at each step. Animals were handled regularly by the experimenter and habituated to the experimental conditions to avoid other stresses. All experiments were accomplished during the light period of the day.

### 2.2. Noise procedure

Broadband white noise at 100dB intensity was produced by a white noise generator (Brüel & Kjære, Germany), amplified by an amplifier connected to a loudspeaker fixed 30cm above the animal cage. A hand held sound level meter (Brüel & Kjære, Germany) was used to measure the intensity of the noise. To avoid effects of acute noise stress, the 15 days and 30 days exposed group animals were sacrificed on the day after their final exposure to noise.

### 2.3. Spatial memory test

Spatial memory is a navigational memory depending on the spatial orientation and generally tested using MWM test procedure (n = 10 rat/group). The environmental conditions (temperature, humidity, light, and sound) were properly maintained, and the test was performed as per the protocol reported elsewhere (Shukla et al., 2019). After completion of 15 days and 30days noise exposure, rats immediately underwent the test phase (with hidden platform and without hidden platform) in which they were again placed opposite to ISLAND zone, i.e., Z2 zone for 1 min.

Latency, path length and path efficiency to reach the platform (with the platform hidden), number of entries and time spent in the ISLAND zone (without the platform) were evaluated under probe and spatial memory test.

### 2.4. Blood, tissue collection, and processing

Immediately after the behavioral test, rats were anesthetized with ketamine 80 mg/kg-xylazine 20 mg/kg mixture. Blood was collected from the left ventricle and centrifuged at 3500 rpm for 15 min, plasma was separated and aliquots stored at −80 °C for further analysis.

For dissecting the hippocampus, the whole brain was extracted after anesthetizing the rats by giving ketamine 80 mg/kg: xylazine 20 mg/kg combination. The hippocampus region was isolated from the whole brain, kept on ice, washed with 0.1 M phosphate-buffered saline (PBS) solution and stored at − 80 °C. Hippocampus tissue was sonicated in 1 × PBS solution containing protease inhibitor cocktail and centrifuged at 10,000 rpm for 15 min at 4 °C. The supernatant was separated carefully and stored at − 80 °C for enzyme-linked immunosorbent assay (ELISA).

### 2.5. Biochemical analysis

#### 2.5.1. ROS estimation using DCFHDA

A non-fluorescent lipophilic dye, Dichlorofluorescein diacetate (DCFHDA) **(Cat #C400, Life Technologies, USA)**, was used to measure ROS levels in tissue homogenate of all three groups (n = 5 rat/group). Once internalized into the cells, it is cleaved into 2,7-dichlorofluorescein by intracellular esterase and on combining with ROS, cleaved DCF generates fluorescence. The fluorescence produced is directly proportional to the ROS levels. 10 μl of 10 μM DCFHDA was added to 150 μl of hippocampus tissue homogenate (10% w/v in RIPA buffer, Millipore, USA) and incubated for 40 min at 37 °C in amber tubes (Borosil, USA) in the dark. Finally, fluorescence was measured at 488 nm excitation and 525 nm emission wavelengths, respectively using fluorimeter (LS45 Luminescence Spectrometer, PerkinElmer, USA). The fluorescence units were normalized to background and data was then presented as FU/mg protein.

#### 2.5.2. Lipid per-oxidation status using MDA assay

Briefly, to assess the lipid peroxidation status, 750 μl of trichloroacetic acid (TCA; 20% w/v in distilled water) and 750 μl of thiobarbituric acid (0.67% w/v in 0.05 M NaOH) were added to 250 μl of the hippocampus tissue homogenate each, in series, incubated in a water bath at 95 °C for 15 min and then allowed to cool to room temperature. The mixture was then centrifuged (400 g; 5 min). 200 μl of the supernatant from each group was added in triplicate in a 96-well plate and optical density was measured at 531 nm using spectrophotometer (Versa Max ELISA Microplate Reader). The data was normalized with protein content of the samples estimated using standard Bradford's assay and subsequently represented as μmol MDA/mg of protein.

#### 2.5.3. Estimation of superoxide dismutase activity

Quantification of Superoxide dismutase activity was accomplished using EnzyChrom™ superoxide dismutase assay kit **(Cat # ESOD-100, Bioassay systems, USA)** as per the manufacturer's instructions. In concise form, 20 μl standard or hippocampus tissue homogenate samples were added in triplicate to a 96 well plate. Then 160 μl working reagent containing assay buffer, xanthine and WST-1 were added to each well in given order. Optical density was measured immediately at 430 nm (OD0) and then plate was incubated at 25 °C for 60 min. Again, optical density was measured at 430 nm (OD60). Finally, the concentration of SOD was measured using ΔΔOD vs SOD concentration standard curve. Activity was represented as unit/mg protein.

#### 2.5.4. Estimation of reduced glutathione

Reduced glutathione was measured using EnzyChrom™ GSH/GSSG

Assay kit (**Cat. No. EGTT-100, BioAssay Systems, USA)** in brain hippocampus tissue lysates. Briefly, 25 μl tissue homogenates samples from each group were deproteinated using 65 μl of 5% w/v metaphosphoric acid. About 12 μl of clear supernatant was taken and mixed with 488 μl of 1X Assay buffer. Then, 200 μl of the prepared sample was added to a single well of ELISA 96-well plate and 100 μl Working Reagent (1X Assay buffer, GR enzyme, NADPH & DTNB) was subsequently added. Absorbance was taken immediately and after 10 min at 412 nm.

### 2.5.5. *Estimation of cytokine levels in collected hippocampus and blood plasma*

Cytokine IL-1α (rabbit anti IL-1α Santacruz sc-7929), TNF-α (Mouse anti TNF- Santacruz sc-57315), IL-6 (Anti IL-6 antibody Abcam ab6672), IFN-γ (Mouse anti IFN-γ Santacruz ab22343), IL-4 (Anti IL-4 antibody Abcam ab9622) and Il-10 (Anti-IL-10- antibody, Abcam, ab9969) levels in plasma and hippocampal lysates (n = 6 animals/group for each) were assessed using their respective indirect ELISA methods (Baitharu et al., 2013) and the result calculated as relative fold change.

### 2.6. *Histological analysis*

### 2.6.1. *Morphological analysis of hippocampus using cresyl violet (CV) staining*

CV staining was performed as described earlier (Kumar et al., 2018; Kushwah et al., 2018). Briefly, approximately 20μm coronal sections were sliced using a cryostat (Leica Biosystems). The sections were stained with 0.1% cresyl violet and the morphology of the neurons examined under a light microscope in control and experimental groups (n = 6 animals/group). The small sized, dense, irregular shaped pyknotic cells were considered as dead neurons (Baitharu et al., 2013). The number of pyknotic neurons was counted in a frame of 0.1 mm$^2$ with a 40× objective (total magnification 400x) of both hemispheres of hippocampus using Image J software.

### 2.6.2. *Caspase-3 immunohistochemistry*

Coronal tissue sections of 30 μm thickness from hippocampus (Bregma, −3.60 to −4.52 mm) were collected in PBS as per the method of Paxinos and Watson (2007). Sections were washed thrice with PBST (Phosphate Buffered Saline with Tween20) for 5 min each and were then incubated for 10 min in sodium citrate buffer (10 mM, pH 6.0) at 100 °C for antigen retrieval. After washing thrice with PBST, blocking was done using the blocking buffer (5% bovine serum albumin in 0.1 M PBS and 0.5% Triton X-100) for 2 h at room temperature. Subsequently, sections were treated overnight in 1:500 dilution of caspase 3 antibody (Abcam, USA) prepared in the blocking buffer at 4 °C. After incubation, sections were washed in PBST, followed by 0.3% hydrogen peroxide treatment for 10 min. They were again washed with PBST and then incubated in 1:1000 of Alexa Flour Antibody conjugate Alexa 594 goat anti-rabbit IgG secondary antibody (Sigma, USA) for 2 h at room temperature. This was followed by thorough washing for three times, each of 5 min duration with PBST. All sections were counterstained with DAPI for 5 min at RT and mounted with gold antifade mounting media. Images were captured at 20x using Fluorescence microscope (Olympus BX 51). Caspase 3 positive cells were counted in a frame of 0.1 mm$^2$ using Image Pro-Plus 5.1 image analysis software from both hemispheres of the limbic brain region. Six sections per animal and cells from both the hemispheres were considered for counting (n = 6 animals/group). Apoptotic neurons falling on the boundary line of the rectangular box were excluded to avoid recounting of the same cell.

### 2.6.3. *TUNEL assay*

Apoptosis is a marker for cellular self-destruction due to activation of nucleases that finally degrade the nuclear DNA into fragments of more or less 200 base pairs in length. Detection of these DNA fragments was in tissue obtained after cryo-sectioning directly using TUNEL apoptosis detection kit (Cat# ab206386, Abcam) (n = 5 animals/group).

### 2.7. *PCR array*

### 2.7.1. *RNA isolation and cDNA synthesis*

Total RNA was isolated from hippocampus tissue using TRIzol method. Quantification of RNA was done using Biophotometer plus (Eppendorf) that measured absorbance at 260/280 nm. For genomic DNA contamination elimination used DNAse I. RNA reverse transcription was initiated promptly after quantification of RNA using High capacity RT$^2$ first strand cDNA Synthesis Kit (Qiagen) as per the manufacturer's instructions. The synthesis programme appended a single incubation at 42 °C for 15 min, followed by incubation at 95 °C for 5 min. The reaction volume was made up to 100 μl with MilliQ water. This cDNA was used for Quantitative RT-PCR.

### 2.7.2. *Real time PCR*

To elucidate the expression of 84 genes related to inflammatory cytokines and receptor genes Rat RT$^2$ Profiler™ PCR Array profiling from Qiagen (PARN-011Z, Qiagen, USA) was used for analysis of inflammatory cytokines and receptor specific transcripts as per the manufacturer's guidelines. Briefly, 1248 μl nuclease-free water (AM9937, Ambion, USA), 1350 μl SYBR green master mix (Qiagen) and 102 μl cDNA were mixed in a solution. 25 μl was added to each well of the 96-well array plate from this solution. RT-PCR protocol was set at 95 °C for 10 min. Then 40 cycles were performed with 95 °C for 15 s and 60 °C for 1 min. CFX 96 well Bio-Rad was used for performing the RT-PCR.

### 2.7.3. *Analysis*

CT values were exported to an Excel file to create a table of CT values. This table was then uploaded on to the data analysis web portal at http://www.qiagen.com/geneglobe. Samples were assigned to controls and test groups. CT values were normalized based on a Manual Selection of reference genes. The data analysis web portal calculates fold change/regulation using delta CT method, in which delta CT is calculated between gene of interest (GOI) and an average of reference genes (HKG), followed by delta CT calculations (delta CT (Test Group)-delta CT (Control Group)). Fold Change is then calculated using $2^{-\Delta Ct}$ formula. The data analysis web portal also plots scatter plot, volcano plot, clustergram, and heat map. This data analysis report was exported from the QIAGEN web portal at GeneGlobe.

Protein-protein interactions network was done by STRING 10.0 online web server (http://string.embl.de)

### 2.8. *DATA analysis*

Results are presented as Mean ± Standard Error of Mean (SEM). Behavioral analysis, TUNEL assays, pro/anti-inflammatory cytokines level, oxidative stress and caspase-3 were analyzed using one-way ANOVA followed by Bonferroni's multiple comparison test (GraphPad Prism software).

## 3. Result

### 3.1. *Spatial reference memory during noise exposure*

All experimental rats were trained in MWM for spatial learning assessment to an equivalent level of 'performed to assist' by probe trial and memory test before noise exposure. On day 8 of training, the rats showed non-significant changes in the time spent to reach the platform in the targeted quadrant (during probe trial and memory test). The time spent in the target quadrant as well as the platform crossings was significantly less in the 15 and 30-day noise exposure rats (Fig. 1A–F). Rats subjected to memory test immediately after 15 and 30-day exposure to noise showed a significantly increase in latency (Fig. 1B) and path length (Fig. 1C) with diminished time spent in platform zone (Fig. 1D) and number of crossing (Fig. 1E) when compared to the control group.
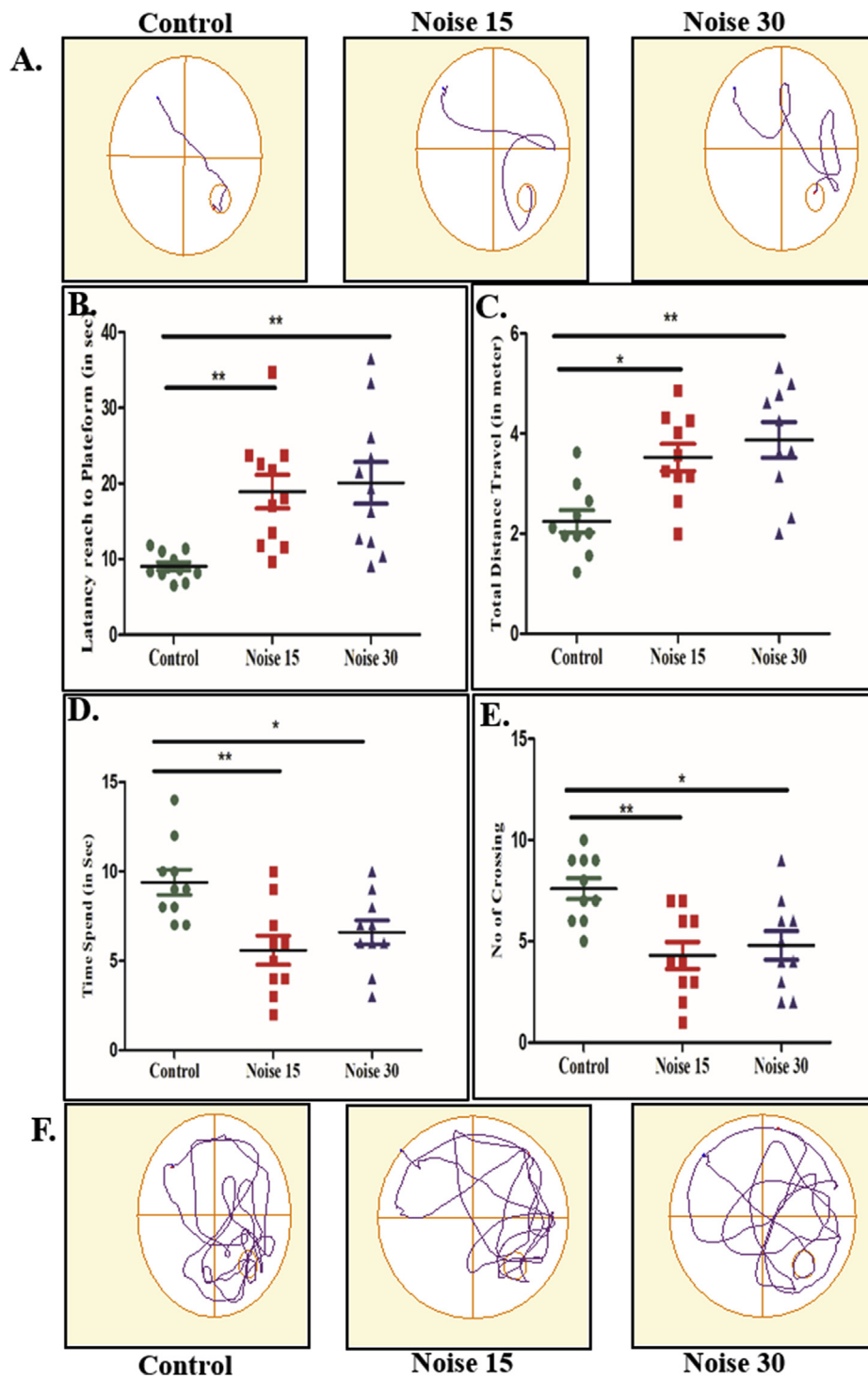
**Fig. 1.** Changes in the different parameters of spatial memory performance in the three categories *viz* control, 15 days noise exposure and 30 days noise exposure. A. Tract plot of spatial memory paradigm (place navigation) B. Latency to reach platform C. Total distance travelled (in mtr) D. Time spend in platform zone E. No. of crossing of platform zone F. Tract plot of spatial memory paradigm (probe trial). One-way ANOVA with Bonferroni post hoc test was used for the analysis of different parameters of MWM performance. Values are represented as Mean $\pm$ SEM (n = 10 animals/group) *p < 0.05, *p < 0.01.

### 3.2. Biochemical parameters

Both the oxidative markers ROS and MDA (a by-product of lipid peroxidation and an important biomarker of membrane damage) in brain hippocampus tissue lysate (Fig. 2A–B) showed significantly increased levels in both the 15 and 30 days noise exposure groups when compared to the control group. At the same time significantly decreased levels of the anti-oxidant SOD and GSH were found in both the exposure groups (Fig. 2C and 2D).

### 3.3. Noise induced abnormal inflammatory changes in hippocampus and plasma

To better understand the stress induced neuro-inflammation due to chronic noise exposure, the hippocampus and plasma of rats were examined for alterations in cytokines using the inflammatory proteins, followed by ELISA analysis. The results suggested that the levels of pro- and anti-inflammatory cytokines was altered in both hippocampus and plasma in exposed rats compared to control. Both day 15 and day 30
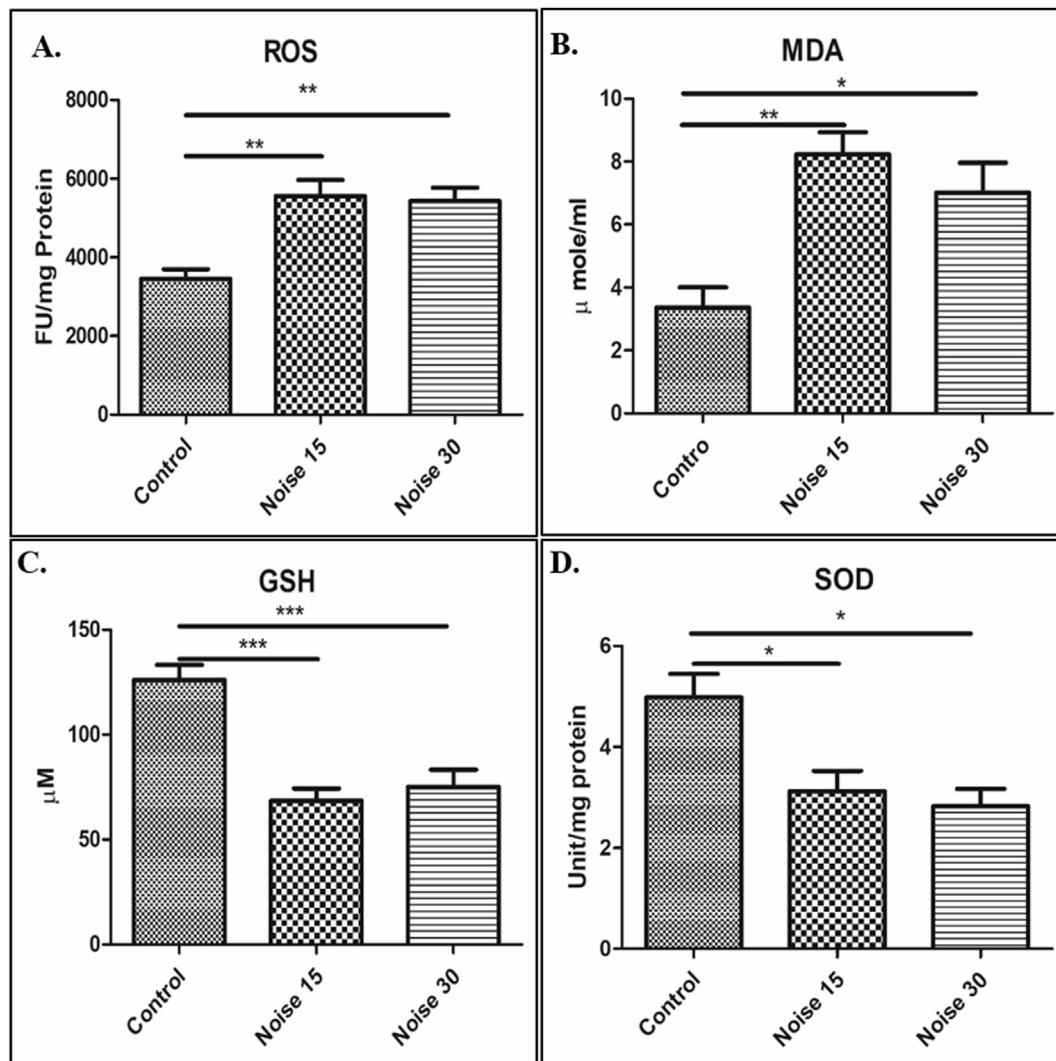
**Fig. 2.** Oxidative stress markers investigated in hippocampus lysate. (A) The formation of reactive oxygen species detected using the fluorescence intensity by 2,7-dichlorofluoroscein diacetate, (B) lipid peroxidation measured as malondialdehyde (MDA) concentration; (C) total glutathione; (D) the content of superoxide dismutase (SOD) activity. One-way ANOVA with Bonferroni post hoc test was used for the analysis of all parameters. Data represents Mean $\pm$ SEM (n = 6 animals/group). *** represents $p < 0.001$, **$p < 0.01$ and * $p < 0.05$ when compared to control and exposure group.

exposed rats showed a significant increase ($p < 0.05$) in the level of pro-inflammatory cytokines i.e., TNF-$\alpha$, IL-1$\alpha$, IFN-$\gamma$, and IL-6 (Fig. 3A–3D) in the hippocampus and the plasma of rats when compared with their non-exposed counterparts. Simultaneously, the levels of anti-inflammatory cytokines; IL-4 and IL-10 (Fig. 3E and 3F) significantly decreased ($p < 0.05$) after noise exposure (day 15 and day 30) in both hippocampus and plasma compared with controls.

### 3.4. Noise induced changes of neuronal morphology in hippocampus region

To explicate the effect of noise on hippocampus neuronal morphology, the appropriate sections were stained with cresyl violet (Nissl staining). Following 15 and 30 days of exposure to noise, significant pyknosis was observed in DG (Fig. 4I, J, 4K), CA3(Fig. 4E, F, 4G) and CA1(Fig. 4A, B, 4C) regions of hippocampus when compared to the control group. Overall, the neuronal morphology results suggest that maximum changes were effected at 15-day noise exposure (Fig. 4B, F, 4J).

### 3.5. Caspase-3 positive neuron count in hippocampus after noise exposure

Significant increase, with respect to controls, in active Caspase-3 positive neurons was observed in the15 days and 30 days exposure

groups in DG (Fig. 5D and G) regions of hippocampus. No significant difference was noticed between the15 and 30 days exposure groups. Significant positive correlation of C3 positive count in hippocampus with memory impairment was seen ($r^2 = 0.3906$; *$p < 0.05$, Fig. 5E).

### 3.6. Noise induced neuronal DNA fragmentation in brain region

One of the main features of apoptosis is DNA damage. Accordingly, the nuclear morphology of apoptotic neuronal cells was visualized with TUNEL staining which is an assay for DNA breaks based on enzymatic labeling of free 3′ DNA ends. Both 15 and 30 days noise exposures significantly increased the number of TUNEL-positive neurons compared with control (**$p < 0.001$, $p < 0.01$, $p < 0.05$**, Fig. 6A–6F).

### 3.7. Noise induced alterations in inflammatory related genes RT$^2$-PCR array experiments

Commercial RT$^2$PCR expression array was used to determine changes in the expression of 84 inflammatory and cytokines receptors related genes. Up regulation ($\geq$2.0fold expression change) of gene expression in day 15 noise exposure group was observed in respect of genes *Il17f, Ccl6, Tnfsf4, Tnfsf13b, Cxcr5, Il16, Ccl9, Ccr2, Ccr3, Cxcl12, Tnfrsf11b, Il2rg,*
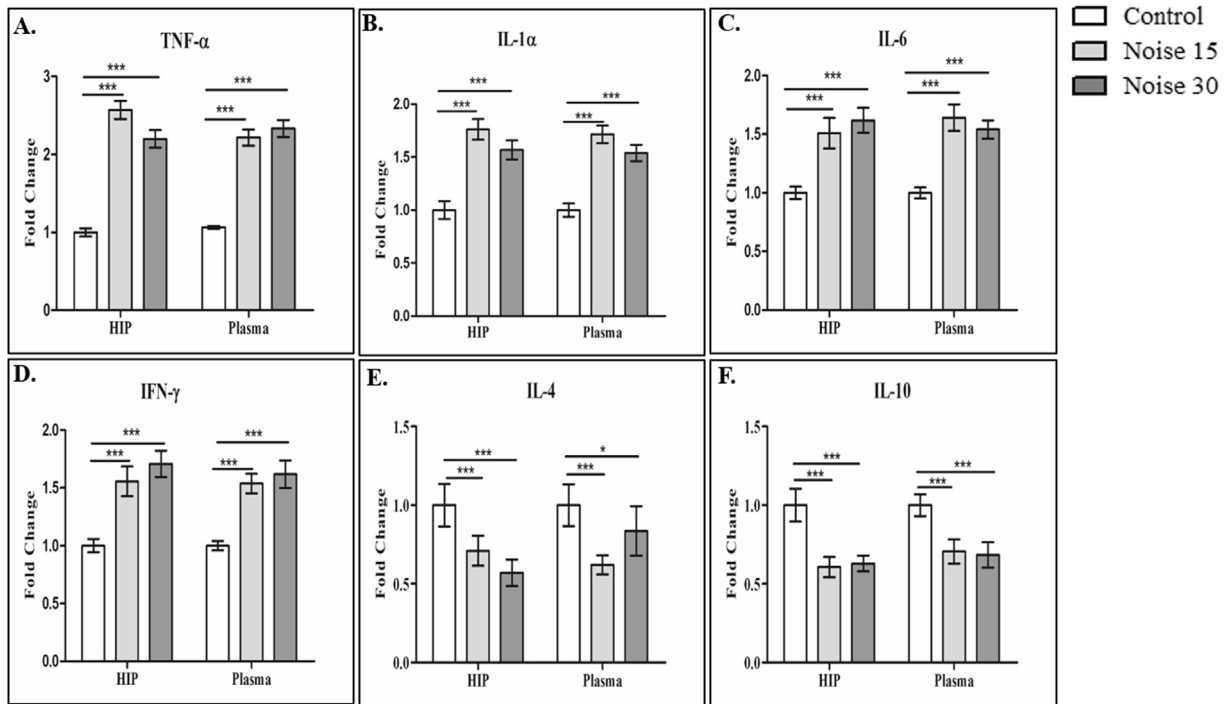
**Fig. 3.** Fold changes in the inflammatory cytokines in hippocampus and plasma following noise exposure. The cytokine levels were expressed as fold changes in A: TNF-α; B: interleukin-1α(IL-1α); C: IL-6 (pro-inflammatory cytokines); D: IFN-γ; E: IL-4; F: IL-10 (anti-inflammatory cytokines) in the hippocampus and plasma. Data represents Mean ± SEM (n = 6 animals/group). *represents p < 0.05; **p < 0.01; ***p < 0.001 when compared to control with noise exposure group. One-way ANOVA with Bonferroni post hoc test was used for the analysis of different cytokines parameters.
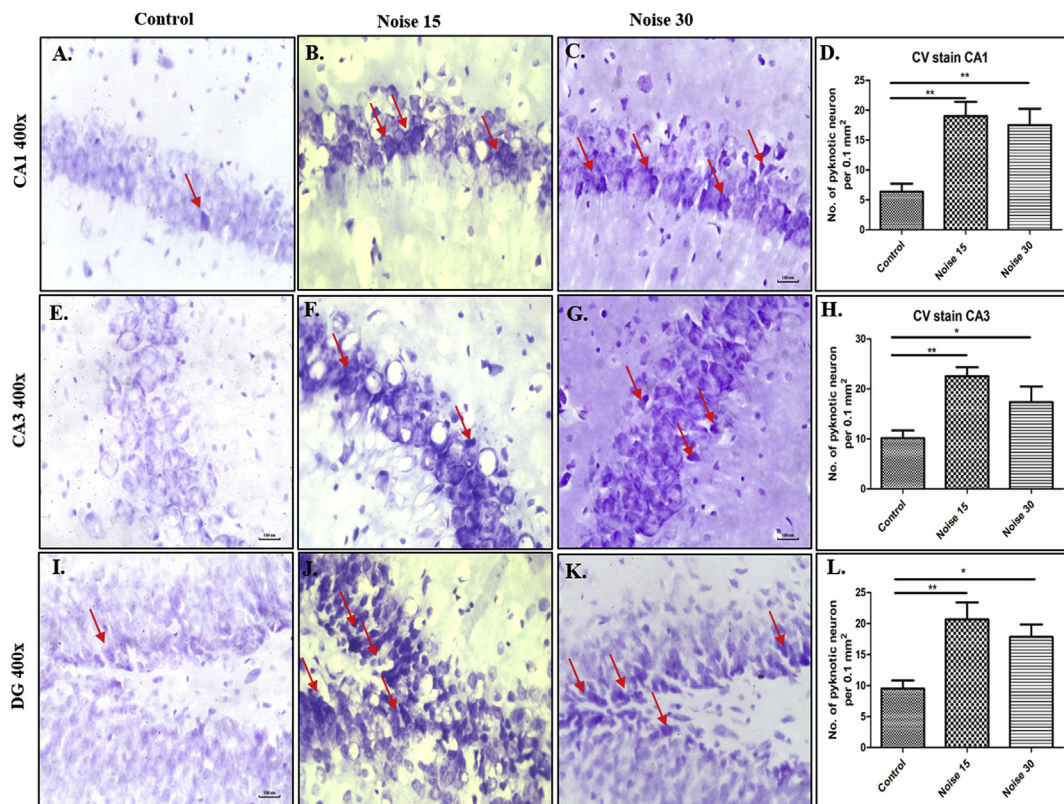


**Fig. 4.** This figure represents change in number of pyknotic cells in CA1, CA3 and DG region of hippocampus through Cresyl Violet staining in following groups: Control: A. CA1; E. CA3; I. DG; Day 15 Exposure: B. CA1; F. CA3; J. DG; Day 30 Exposure: C. CA1; G. CA3; K. DG group; D: graphical representation of total number of pyknotic neuron in CA1 region; H: graphical representation of total number of pyknotic neuron in CA3 region L: graphical representation of total number of pyknotic neuron in DG region. One-way ANOVA with Bonferroni post hoc test was used for the analysis of all parameter. Data represents Mean ± SEM (n = 6 animals/group). **represents p < 0.01 and * p < 0.05 when compared to control and exposure group.
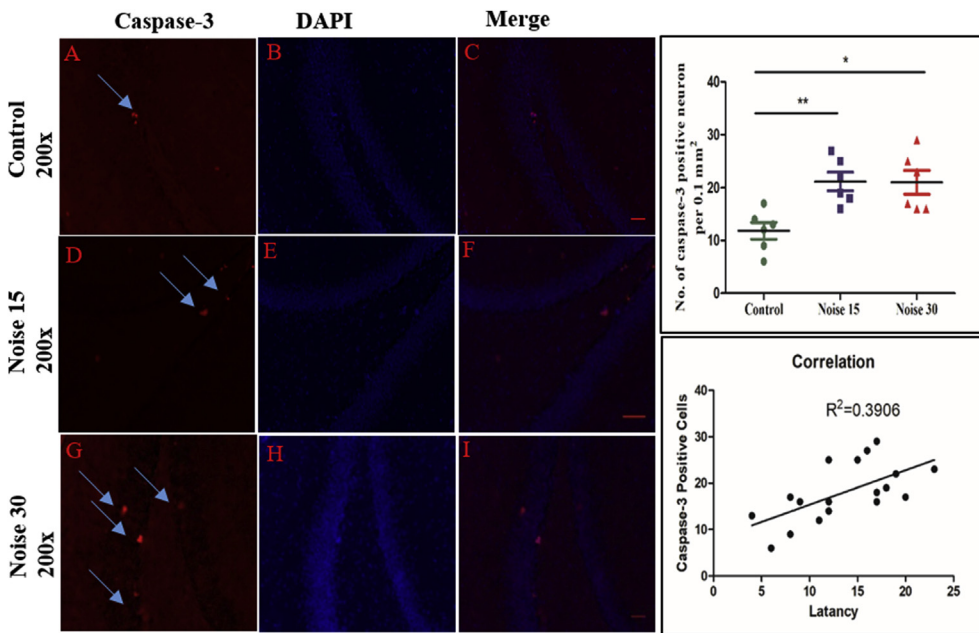
**Fig. 5.** Change in Caspase 3 positive cells in the rat hippocampus A: in the normal rat, caspase-3 positive cells (arrowheads) form a thin line in dentate gyrus (DG) region. B, C: DAPI stain and Merged image of control group; D, G: noise 15 and noise 30 days exposed rats exhibited highly expressed number of Caspase-3 positive cells; E, F, H, I: DAPI stain and Merged image of noise 15 and noise 30 days exposed group respectively; J: graph bar representation of total number of Caspase-3 positive cells. One-way ANOVA with Bonferroni post hoc test was used for the analysis of positive Caspase-3 positive cells count. The values are represented as Mean $\pm$ SEM (n = 6 animals/group) **p < 0.01, *p < 0.05. Pearson's correlation test followed by linear regression was performed for correlation analysis.
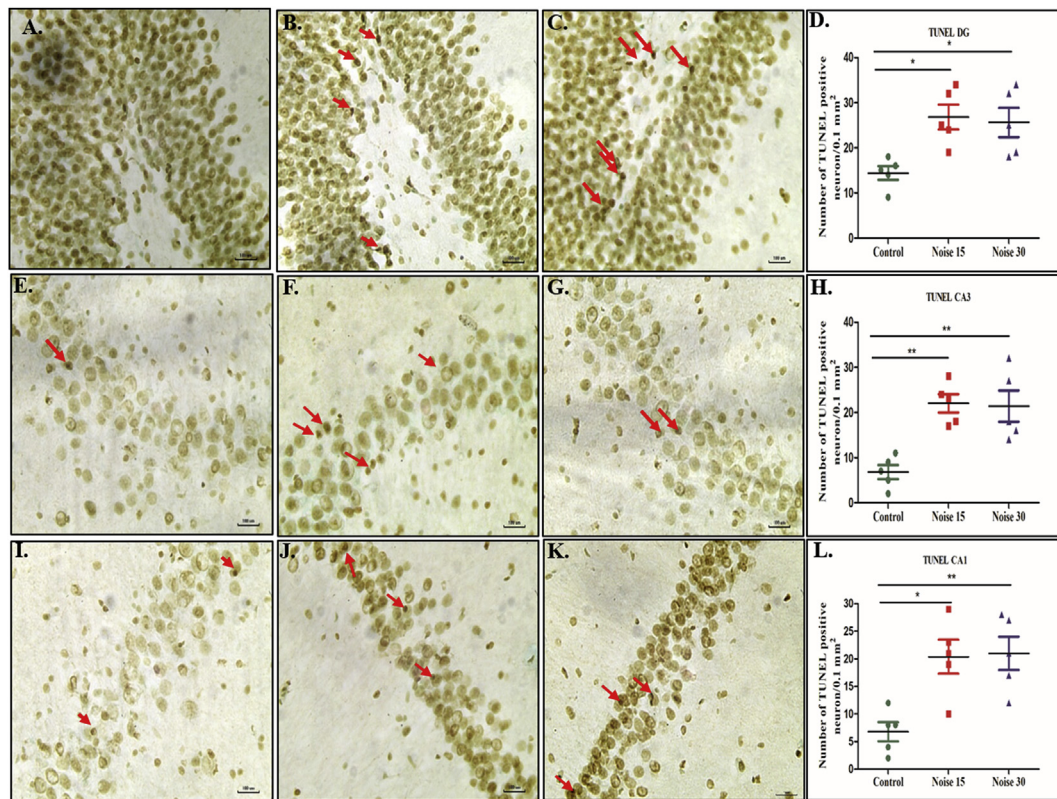


**Fig. 6.** This figure represents change in number of apoptotic cells in CA1, CA3 and DG region of hippocampus through TUNEL staining. A. DG; B. CA3; C. CA1 regions. D. E. F. graph bar representation of total number of TUNEL positive cells in DG, CA3, CA1 respectively. One-way ANOVA with Bonferroni post hoc test was used for the analysis of positive TUNEL positive cells count. Data represents Mean $\pm$ SEM (n = 5 animals/group). *** represents p < 0.001, **p < 0.01 and * p < 0.05 when compared to control and exposure group.

*Ccl7, Il1a, Il5, Cxcl6, Ccr5, Ccl20, Cxcr1, Ccr1, Il13, Tnf, Ccl2, Il17 a while* genes *il3, bmp2* showed down regulation. Similarly, in day 30 noise exposure group genes *Cx3cl1, Il2rg, Tnfsf4, Ccl22, Osm, Ccr1, Tnfsf14, Il1a, Tnfrsf11b, Cxcr5, Tnf, Ccl2, Il17a, Cxcr1, Ccr2, Il13* were up regulated and *Bmp2, Il3, Il4, Tnfsf11* were down regulated at relative fold change as shown in Fig. 7F-7AF. Of the five housekeeping genes *actb, b2m, ldha* and *rplp1* were stable, with an average fold change equal or less than $\pm 0.37$ fold, at all the three time points viz. Control, day 15 and day 30 exposures. The remaining gene (*hprt 1*) showed fold changes at one-time point. Accordingly, the average of *actb, b2m, ldha* and *rplp1* only was used to normalize the expression levels of inflammatory and cytokines receptor related genes. The constitutive expression level of the
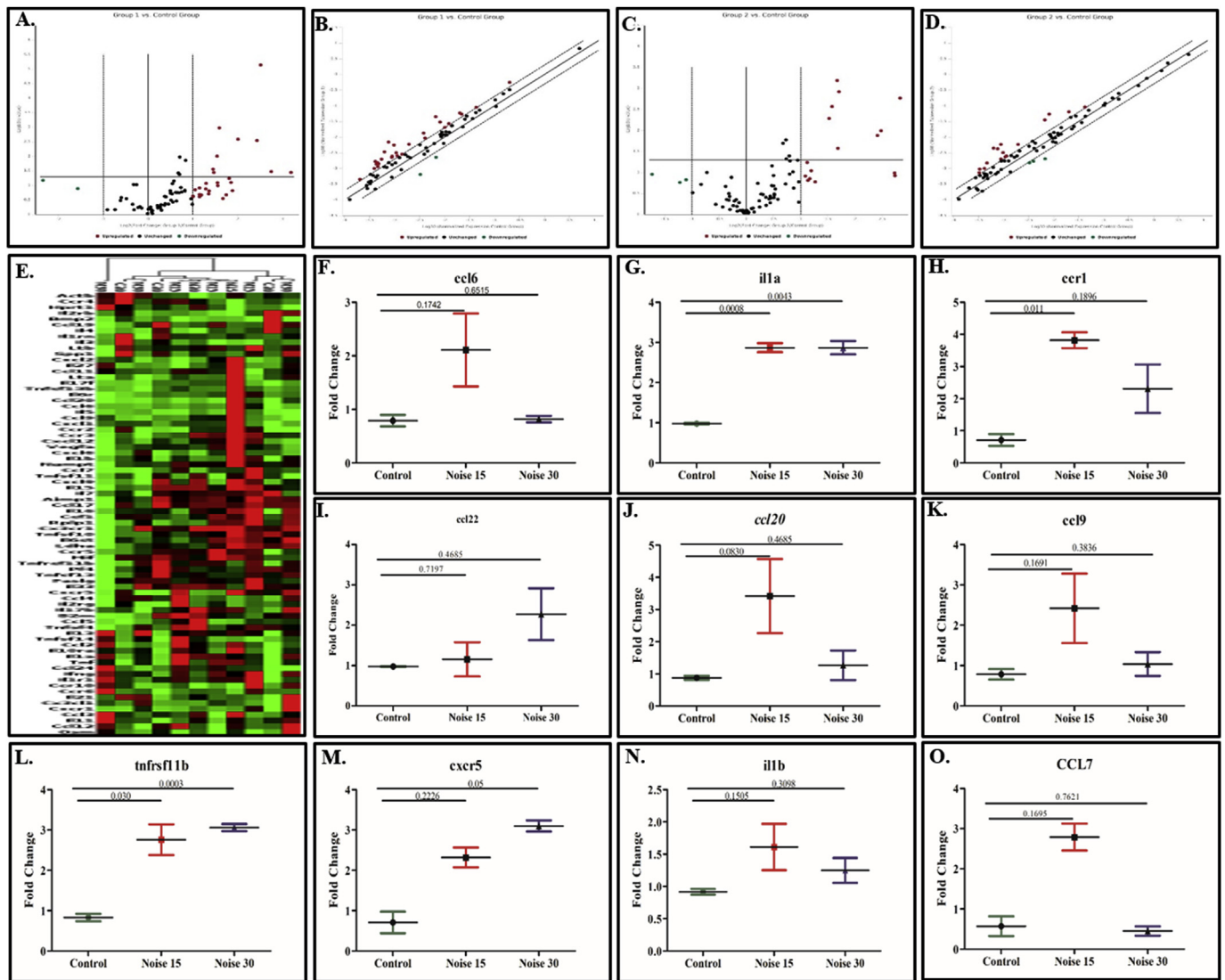
**Fig. 7.** Heat-map comparison of 84 inflammatory cytokines and receptors gene in brain tissue hippocampus lysate Control, Noise 15 days and day 30 after noise exposure for 2 h, 100dB (n = 3 animals/group). Genes were displayed for fold-change variation in respect to their control groups and coloured by their normalized expression value (red: high expression; green: low expression). Figure 7F-7AF showed multiple genes with p-value change compared with control. Fig. 7A volcano plot for noise 15; 7C for noise 30 compared with control. Fig. 7B & D for scatter plot for noise 15 and noise 30 respectively. Fig. 7A–D Genes upregulated with fold change greater than 2 and are represented as red dots; genes with fold change less than 0.5 are shown as green dots; unmodulated genes are shown as black. Fig. 7E Heat map detailed display of all upregulated genes for Control, day 15 noise exposure, and day 30 noise exposure group. (For interpretation of the references to colour in this figure legend, the reader is referred to the Web version of this article.)

inflammatory related genes was evaluated in the controls (3 biological replicates). Using the average expression level of the three stable housekeeping genes (*actb, b2m, ldha and rplp1*) as reference, the relative expression levels of inflammatory-related genes were calculated. Table 1. Presents the fold differences with control in noise 15 and noise 30.

### 3.8. Bioinformatics networking by STRING 10.0 online web server

STRING database was employed for collection and dissemination of information associated with cellular functional interaction between differentially expressed proteins. Integration of protein-protein interaction includes direct (physical) interaction and indirect (function) interaction as both are specific and biologically relevant. These associations are derived from genomic context, co-expression, and text mining.

In the present study, the proteins exhibiting statistically significant changes were submitted into the online web server STRING 10.0 to analyze interactions among all the proteins (Fig. 8). The confidence score

is considered for representing protein-protein interactions. According to STRING 10.0, 0.15, 0.4 and 0.7 score indicates lowest, medium and highest confidence respectively. Proteins undergoing significant changes during noise exposure were submitted and it was discerned that 11 participating proteins had a high confidence and highest confidence interaction i.e. >0.700 confidence level. As per the score result, tnf, il13, ccl2, ccr5, cxcl6, il1a, cxcr1, pf4, spp2, bmp2 and il4 showed high confidence, which demonstrates that the above stated proteins are closely associated with noise induced inflammation and cognitive decline.

For the cellular component category: most of the proteins were primarily localized in extracellular region. For biological process: regulation of signaling receptor activity, inflammatory response, immune response, immune system process, cytokine-mediated signaling pathway; and for molecular function category: regulation of signaling receptor activity, inflammatory response, immune response, immune system process, cytokine-mediated signaling pathway etc. Were detected. Collectively, the results as provided in Table 2 suggested that the proteins that were
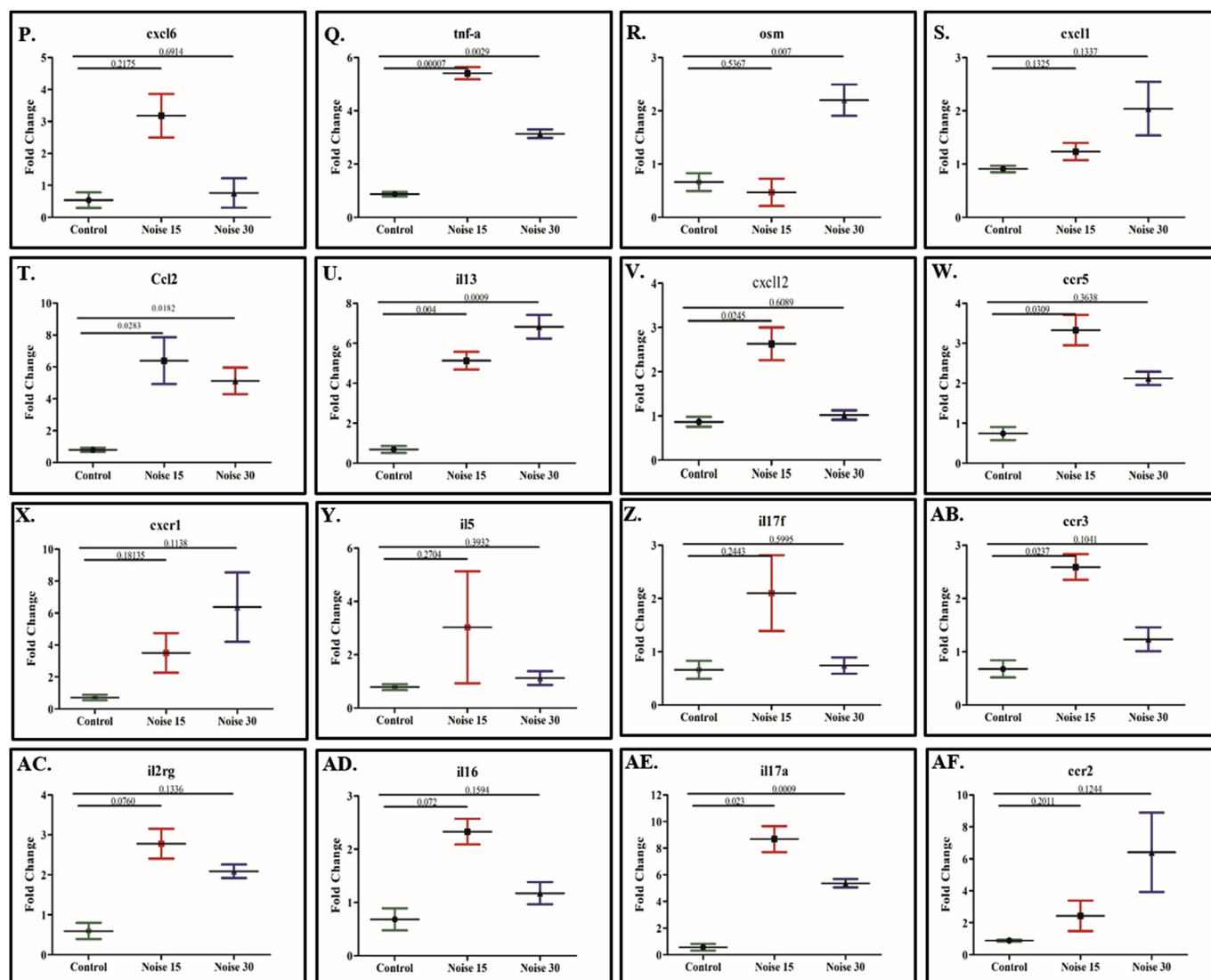
**Fig. 7.** (*continued*).

expressed significantly upon exposure to noise environment were mainly associated with stress and inflammatory pathways.

## 4. Discussion

This study demonstrates the effects of moderate intensity noise exposures on hippocampus through behavioral, biochemical and morphological analyses. It was discerned that noise affected spatial learning and memory through increase in oxidative stress and inflammation as evinced by elevated levels of TNF-α, IL-6, IL-1α and IFN-γ in both hippocampus and plasma. Additionally, exposure to noise resulted in gradual increase in the number of pyknotic and apoptotic neurons in CA1, CA3 and DG regions along with an increase in DNA fragmentation in DG region of hippocampus.

MWM test was undertaken to assess the deleterious effects of noise stress on spatial learning and memory. Performance in MWM involves several components including concept formation, attention, working memory and reference memory. The hidden platform test and probe trial test are most specific for observing the effects on spatial learning and memory respectively (Morris et al., 1982). Our findings revealed that moderate intensity noise exposure impaired early memory in the probe trial, and learning as indicated by hidden platform task. An increase in the pro-apoptotic protein caspase-3 was observed in the hippocampus of

rats exposed to loud noise. This observation is in concert with previous reports where similar conclusions were drawn (Kim et al., 2013). These findings indicate that noise is able to modulate the apoptotic pathway, producing a final effect, which depends on the intensity and duration of exposure.

Our present studies also indicated increase in oxidative stress with enhanced levels of ROS and MDA on noise exposures, with concomitant decrease in the levels of antioxidants SOD and GSH. Results suggested that noise exposure may increase ROS levels with induction of pro-inflammatory response as demonstrated with the specific markers TNF-α, IL-6, IFN-γ etc. In hippocampus. Earlier studies (Uran et al., 2010) have proven that effects of noise on ROS within brain areas increment cerebellar ROS amount and catalase activity in hippocampus in rats exposed for 2 h to 95–97 dB. Chronic impairment of spatial and associative memory was observed earlier in noise-exposed rats (Uran et al., 2010) where it was suggested that such an effect was dependent on the imbalance of oxidative status in hippocampus and cerebellum, which were involved in memory processing. Likewise, our studies indicated that noise stress led to increased ROS and MDA levels, memory impairment and decline in the levels of GSH and SOD in hippocampus in both the noise exposed groups. As such, lipid peroxidation incited by MDA was plausibly responsible for cellular toxicity in the hippocampus by cross-linking protein and nucleic acids consequent on noise exposure

**Table 1**

Fold-Regulation represents fold-change results in a biologically meaningful way. Fold-change values greater than one indicates a positive- or an up-regulation, and the fold-regulation is equal to the fold-change. Fold-change values less than one indicate a negative or down-regulation, and the fold-regulation is the negative inverse of the fold-change. The p-values are calculated based on one way ANOVA of the replicate 2(- Delta CT) values for each gene in the control group and exposure groups.

| Noise 15 | | | Noise 30 | | |
|---|---|---|---|---|---|
| Gene symbol | Fold regulation | p-value | Gene symbol | Fold regulation | p-value |
| Ccl2 | 6.39 | **0.028389** | Ccl2 | 5.12 | **0.018273** |
| Ccl20 | 3.42 | 0.083065 | Ccl22 | 2.16 | 0.16009 |
| Ccl6 | 2.11 | 0.174296 | Ccr1 | 2.31 | 0.189622 |
| Ccl7 | 2.79 | 0.169541 | Ccr2 | 6.41 | 0.124484 |
| Ccl9 | 2.42 | 0.169105 | Cx3cl1 | 2.04 | 0.133762 |
| Ccr1 | 3.82 | **0.011036** | Cxcr5 | 3.1 | 0.057949 |
| Ccr2 | 2.44 | 0.201156 | Il13 | 6.83 | **0.000935** |
| Ccr3 | 2.59 | **0.023758** | Il17a | 5.37 | **0.009399** |
| Ccr5 | 3.33 | **0.030957** | Il1a | 2.87 | **0.004316** |
| Cxcl12 | 2.63 | **0.024589** | Il2rg | 2.09 | 0.133642 |
| Cxcl6 | 3.18 | 0.217523 | Cxcr1 | 6.37 | 0.113827 |
| Cxcr5 | 2.32 | 0.222642 | Osm | 2.2 | 0.078143 |
| Il13 | 5.12 | **0.004785** | Tnf | 3.14 | **0.002994** |
| Il16 | 2.33 | 0.073214 | Tnfrsf11 b | 3.06 | **0.003084** |
| Il17a | 8.68 | **0.023069** | Tnfsf14 | 2.76 | **0.015615** |
| Il17f | 2.1 | 0.244397 | Tnfsf4 | 2.11 | 0.278721 |
| Il1a | 2.87 | **0.000899** | Bmp2 | −3.46 | 0.15844 |
| Il2rg | 2.78 | 0.076007 | Il3 | −2.25 | 0.154882 |
| Il5 | 3.03 | 0.270426 | Il4 | −2.43 | 0.2041 |
| Cxcr1 | 3.51 | 0.181352 | Tnfsf11 | −2.07 | 0.1983 |
| Tnf | 5.41 | **0.000072** | | | |
| Tnfrsf13 b | 2.76 | **0.030905** | | | |
| Tnfsf13 b | 2.16 | 0.228074 | | | |
| Tnfsf4 | 2.11 | 0.27275 | | | |
| Bmp2 | −3.15 | 0.170397 | | | |
| Il3 | −5.39 | 0.071719 | | | |

**Table 2**

Gene ontology of the significantly expressed presenting enriched component, process and pathway.

| Biological Process (GO) | | | |
|---|---|---|---|
| GO-term | Description | count in gene set | false discovery rate |
| GO:0010469 | regulation of signaling receptor activity | 19 of 325 | 5.01E-24 |
| GO:0006954 | inflammatory response | 18 of 250 | 5.01E-24 |
| GO:0006955 | immune response | 18 of 386 | 3.04E-21 |
| GO:0002376 | immune system process | 20 of 654 | 9.52E-21 |
| GO:0019221 | cytokine-mediated signaling pathway | 14 of 138 | 1.88E-20 |
| **Molecular Function (GO)** | | | |
| GO:0005125 | cytokine activity | 19 of 93 | 6.05E-35 |
| GO:0005126 | cytokine receptor binding | 15 of 120 | 1.51E-24 |
| GO:0008009 | chemokine activity | 6 of 19 | 7.74E-12 |
| GO:0005515 | protein binding | 21 of 3019 | 8.65E-11 |
| GO:0048020 | CCR chemokine receptor binding | 5 of 14 | 3.02E-10 |
| GO:0004950 | chemokine receptor activity | 4 of 10 | 1.93E-08 |
| GO:0005164 | tumor necrosis factor receptor binding | 3 of 13 | 5.82E-06 |
| **Cellular Component (GO)** | | | |
| GO:0005615 | extracellular space | 20 of 631 | 1.33E-21 |

(Cheng et al., 2011).

Nissl bodies are extracellular RNA granules and sites of protein synthesis, which generally dissolve and disappear in pathological conditions. Current studies have displayed impairments of Nissl bodies in hippocampus of rat models exposed to moderate intensity noise, indicating decline in neuronal function after noise stress. This might have been due to noise induced pathology, such as excitotoxicity in hippocampus.

There is increasing evidence that neuro-inflammation and stress induced pathophysiology are related events (Ceulemans et al., 2010). Pro-inflammatory cytokines are known to be elevated in several
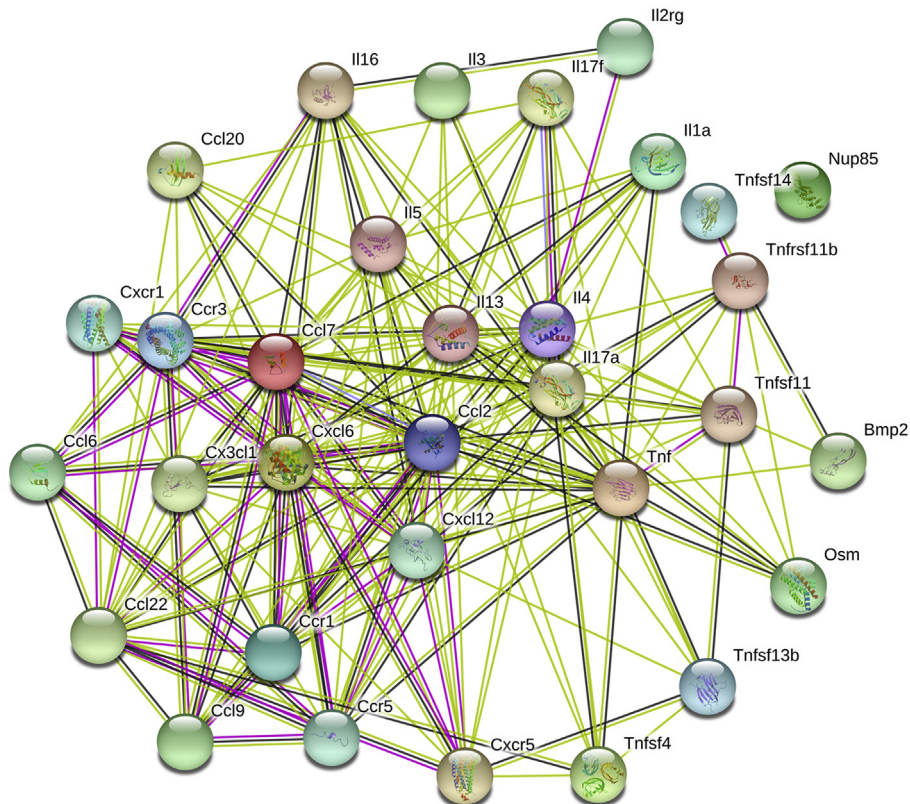


**Fig. 8.** The network analysis of proteins/gene differentiated expressed in noise exposed group.

neuro-pathological conditions associated with deficits in learning memory, and can amplify the generation of additional cytokines, glutamate and oxidative stress (Wang et al., 2012; Yan et al., 1996). The correlation between cytokines and neuro-inflammation is well established in terms of an increased release of pro-inflammatory cytokines in the brain hence, causing memory impairment (Austin et al., 2015). Thus, the imbalance in cytokine (increased pro-inflammatory, decreased anti-inflammatory) levels in both hippocampus and plasma is reflective of a possible interaction between the cytokines and spatial memory during noise exposure. In the current study, we observed a significant elevation in the levels of TNF-$\alpha$, IL-1$\alpha$, IL-6, IFN-$\gamma$ in the hippocampus of noise exposed rats, indicative of enhancement of these important inflammatory factors in response to 15 and 30 days of noise-induced stress in consonance with earlier reports of stress induced inflammation in brain by several researchers (Cui et al., 2015; García-Bueno et al., 2005; Madrigal et al., 2002). Our findings suggest that noise exposure may influence the local cytokines environment in the hippocampus.

The hippocampus region of brain is responsible for the spatial memory (Knapska et al., 2012; LeDoux, 2000; Shukla et al., 2019). Accordingly, our experiments were specially designed to assess neuro-degeneration in this brain region. Our results revealed that noise exposures caused significant pyknosis, apoptosis in DG, CA3 and CA1 regions and DNA fragmentation in the DG region of hippocampus, the latter proven by TUNEL assay.

The present studies suggest that noise stress induces oxidative stress, enhances lipid peroxidation and causes deceleration of ATP production in the mitochondria and release of cytochrome-c. Cytochrome-c then indirectly activates some proteases like caspases (caspase 3, 9) and nucleases like DNase, leading to DNA fragmentation in hippocampus and cortical regions. These changes lead to destabilization of neural circuits in hippocampus and cortical region (Kushwah et al., 2018). These results are consistent with reports by previous researchers which suggested that glutamate excitotoxicity, calcium overloading, oxidative stress and neurodegeneration in the brain regions regulate spatial memory (Baitharu et al., 2013).

Chemokines that are chemotactic for macrophages such as MCP-1/CCL2, MCP-5/CCL12 are unregulated in hippocampus of rats in noise exposed group. Activation of these cell types induces release of cytokines such as IL-1$\beta$, IL-6 and TNF in high concentrations (Whitehead et al., 2010). The aforementioned inflammatory cytokines secreted mainly by microglia, Th1 lymphocytes and M1 phenotype monocytes/macrophages promote neuro-inflammation (Haroon et al., 2012). Cytokines and chemokines, such as MCP-1/CCL2 can act on neurons (Austin and Moalem-Taylor, 2010). MCP-1/CCL2 attracts monocytes to the brain where they enter the brain parenchyma as activated macrophages, capable of producing TNF-$\alpha$ as well as additional inflammatory mediators such as other inflammatory cytokines and reactive nitrogen and oxygen species (Haroon et al., 2012). The chemokine CCL2 is upregulated in the brain during several neurodegenerative and acute diseases associated with infiltration of peripheral leukocytes. Astrocytes can respond to inflammatory cytokines like IL-1$\beta$ and TNF-$\alpha$ by producing chemokines (Conductier et al., 2010; Thompson and Van Eldik, 2009). Other inflammation related genes include chemokine (C-X-C motif) ligand 1 (CxCl1), tumor necrosis factor receptor superfamily member 1a and 1 b (Tnfrf1a, Tnfsf1b), and TNF receptor-associated factor-2 and -4 (Traf2, Traf4). Cxcl1 is up-regulated with inflammation (MacArthur et al., 2011). Tnfr1a, Tnfr1b, and Traf4 are up-regulated on account of apoptosis induced by noise (MacArthur et al., 2013). Ccl5, a chemo-attractant for blood monocytes, memory T-helper cells and eosinophils, causes the release of histamine from basophils and activates eosinophils that may further activate several chemokines and their receptors namely, CCR1, CCR3, CCR4 and CCR5 to play an essential role in neurodegenerative diseases (Liu et. al. 2019).

## 5. Conclusion

In summary, the results of MWM test study demonstrated the deleterious effects of noise exposure on spatial memory. Elevated neuro-inflammatory cytokines evoke inflammatory pathways in hippocampus which happen to be correlated with neuronal dysfunction. These changes in turn instigate cognitive deficits. In light of this, the present study provided substantial evidence to the non-auditory effect of noise exposure on the central nervous system (CNS) and the subsequent results might be helpful for further investigating the underlying neuro-pathological mechanisms.

## Declaration of competing interest

The authors declare that they have no competing interests, financial and otherwise.

## Acknowledgments

## References

Austin, P.J., Berglund, A.M., Siu, S., Fiore, N.T., Gerke-Duncan, M.B., Ollerenshaw, S.L., Leigh, S.-J., Kunjan, P.A., Kang, J.W.M., Keay, K.A., 2015. Evidence for a distinct neuro-immune signature in rats that develop behavioural disability after nerve injury. J. Neuroinflammation 12, 96. https://doi.org/10.1186/s12974-015-0318-4.

Austin, P.J., Moalem-Taylor, G., 2010. The neuro-immune balance in neuropathic pain: involvement of inflammatory immune cells, immune-like glial cells and cytokines. J. Neuroimmunol. 229, 26–50. https://doi.org/10.1016/j.neuroim.2010.08.013.

Baitharu, I., Jain, V., Deep, S.N., Hota, K.B., Hota, S.K., Prasad, D., Ilavazhagan, G., 2013. Withania somnifera root extract ameliorates hypobaric hypoxia induced memory impairment in rats. J. Ethnopharmacol. 145, 431–441. https://doi.org/10.1016/j.jep.2012.10.063.

Balaban, R.S., Nemoto, S., Finkel, T., 2005. Mitochondria, oxidants, and aging. Cell 120, 483–495. https://doi.org/10.1016/j.cell.2005.02.001.

Brown, G.C., Borutaite, V., 2001. Nitric oxide, mitochondria, and cell death. IUBMB Life 52, 189–195. https://doi.org/10.1080/15216540152845993.

Ceulemans, A.-G., Zgavc, T., Kooijman, R., Hachimi-Idrissi, S., Sarre, S., Michotte, Y., 2010. The dual role of the neuroinflammatory response after ischemic stroke: modulatory effects of hypothermia. J. Neuroinflammation 7, 74. https://doi.org/10.1186/1742-2094-7-74.

Cheng, L., Wang, S.-H., Chen, Q.-C., Liao, X.-M., 2011. Moderate noise induced cognition impairment of mice and its underlying mechanisms. Physiol. Behav. 104, 981–988. https://doi.org/10.1016/j.physbeh.2011.06.018.

Conductier, G., Blondeau, N., Guyon, A., Nahon, J.-L., Rovère, C., 2010. The role of monocyte chemoattractant protein MCP1/CCL2 in neuroinflammatory diseases. J. Neuroimmunol. 224, 93–100. https://doi.org/10.1016/j.neuroim.2010.05.010.

Cui, B., Li, K., Gai, Z., She, X., Zhang, N., Xu, C., Chen, X., An, G., Ma, Q., Wang, R., 2015. Chronic noise exposure acts cumulatively to exacerbate alzheimer's disease-like amyloid-$\beta$ pathology and neuroinflammation in the rat Hippocampus. Sci. Rep. 5, 12943. https://doi.org/10.1038/srep12943.

Cui, B., Zhu, L., She, X., Wu, M., Ma, Q., Wang, T., Zhang, N., Xu, C., Chen, X., An, G., Liu, H., 2012. Chronic noise exposure causes persistence of tau hyperphosphorylation and formation of NFT tau in the rat hippocampus and prefrontal cortex. Exp. Neurol. 238, 122–129. https://doi.org/10.1016/j.expneurol.2012.08.028.

Daniel, P., 1984. In: Ramsey, J.M. (Ed.), Basic Pathophysiology. Modern Stress and the Disease Process, vol. 69, pp. 397–398. https://doi.org/10.1113/expphysiol.1984.sp002815, 555. (Addison-Wesley, 1982.) Paperback. £13.25. Q. J. Exp. Physiol.

Denk, A., Wirth, T., Baumann, B., 2000. NF-$\kappa$B transcription factors: critical regulators of hematopoiesis and neuronal survival. Cytokine Growth Factor Rev. 11, 303–320. https://doi.org/10.1016/S1359-6101(00)00009-5.

García-Bueno, B., Madrigal, J.L.M., Lizasoain, I., Moro, M.A., Lorenzo, P., Leza, J.C., 2005. Peroxisome proliferator-activated receptor gamma activation decreases neuroinflammation in brain after stress in rats. Biol. Psychiatr. 57, 885–894. https://doi.org/10.1016/j.biopsych.2005.01.007.

Haroon, E., Raison, C.L., Miller, A.H., 2012. Psychoneuroimmunology meets neuropsychopharmacology: translational implications of the impact of inflammation on behavior. Neuropsychopharmacology 37, 137–162. https://doi.org/10.1038/npp.2011.205.

Kang, S.S., Kurti, A., Fair, D.A., Fryer, J.D., 2014. Dietary intervention rescues maternal obesity induced behavior deficits and neuroinflammation in offspring. J. Neuroinflammation 11, 156. https://doi.org/10.1186/s12974-014-0156-9.

Keithley, E.M., Wang, X., Barkdull, G.C., 2008. Tumor necrosis factor α can induce recruitment of inflammatory cells to the cochlea. Otol. Neurotol. 29, 854–859. https://doi.org/10.1097/MAO.0b013e31818256a9.

Kim, B.-K., Ko, I.-G., Kim, S.-E., Kim, C.-J., Yoon, J.-S., Baik, H.-H., Jin, B.-K., Lee, C.-Y., Baek, S.-B., Shin, M.-S., 2013. Impact of several types of stresses on short-term memory and apoptosis in the Hippocampus of rats. Int. Neurourol. J. 17, 114–120. https://doi.org/10.5213/inj.2013.17.3.114.

Knapska, E., Macias, M., Mikosz, M., Nowak, A., Owczarek, D., Wawrzyniak, M., Pieprzyk, M., Cymerman, I.A., Werka, T., Sheng, M., Maren, S., Jaworski, J., Kaczmarek, L., 2012. Functional anatomy of neural circuits regulating fear and extinction. Proc. Natl. Acad. Sci. Unit. States Am. 109, 17093–17098. https://doi.org/10.1073/pnas.1202087109.

Kumar, R., Jain, V., Kushwah, N., Dheer, A., Mishra, K.P., Prasad, D., Singh, S.B., 2018. Role of DNA methylation in hypobaric hypoxia-induced neurodegeneration and spatial memory impairment. Ann. Neurosci. 25, 191–200. https://doi.org/10.1159/000490368.

Kushwah, N., Jain, V., Dheer, A., Kumar, R., Prasad, D., Khan, N., 2018. Hypobaric hypoxia-induced learning and memory impairment: elucidating the role of small conductance Ca2+-activated K+ channels. Neuroscience 388, 418–429. https://doi.org/10.1016/j.neuroscience.2018.07.026.

LeDoux, J.E., 2000. Emotion circuits in the brain. Annu. Rev. Neurosci. 23, 155–184. https://doi.org/10.1146/annurev.neuro.23.1.155.

MacArthur, C.J., Hausman, F., Kempton, J.B., Sautter, N., Trune, D.R., 2013. Inner ear tissue remodeling and ion homeostasis gene alteration in murine chronic otitis media. Otol. Neurotol. 34, 338–346. https://doi.org/10.1097/MAO.0b013e31827b4d0a.

MacArthur, C.J., Hausman, F., Kempton, J.B., Trune, D.R., 2011. Murine middle ear inflammation and ion homeostasis gene expression. Otol. Neurotol. 32, 508–515. https://doi.org/10.1097/MAO.0b013e31820e6de4.

Madrigal, J.L.M., Hurtado, O., Moro, M.A., Lizasoain, I., Lorenzo, P., Castrillo, A., Boscá, L., Leza, J.C., 2002. The increase in TNF-alpha levels is implicated in NF-kappaB activation and inducible nitric oxide synthase expression in brain cortex after immobilization stress. Neuropsychopharmacology 26, 155–163. https://doi.org/10.1016/S0893-133X(01)00292-5.

Manikandan, S., Padma, M.K., Srikumar, R., Jeya Parthasarathy, N., Muthuvel, A., Sheela Devi, R., 2006. Effects of chronic noise stress on spatial memory of rats in relation to neuronal dendritic alteration and free radical-imbalance in hippocampus and medial prefrontal cortex. Neurosci. Lett. 399, 17–22. https://doi.org/10.1016/j.neulet.2006.01.037.

Morris, R.G., Garrud, P., Rawlins, J.N., O'Keefe, J., 1982. Place navigation impaired in rats with hippocampal lesions. Nature 297, 681–683. https://doi.org/10.1038/297681a0.

Shukla, M., Roy, K., Kaur, C., Nayak, D., Mani, K.V., Shukla, S., Kapoor, N., 2019. Attenuation of adverse effects of noise induced hearing loss on adult neurogenesis and memory in rats by intervention with Adenosine A2A receptor agonist. Brain Res. Bull. 147, 47–57. https://doi.org/10.1016/j.brainresbull.2019.02.006.

Tan, W.J.T., Thorne, P.R., Vlajkovic, S.M., 2016. Characterisation of cochlear inflammation in mice following acute and chronic noise exposure. Histochem. Cell Biol. 146, 219–230. https://doi.org/10.1007/s00418-016-1436-5.

Thompson, W.L., Van Eldik, L.J., 2009. Inflammatory cytokines stimulate the chemokines CCL2/MCP-1 and CCL7/MCP-3 through NFkB and MAPK dependent pathways in rat astrocytes [corrected]. Brain Res. 1287, 47–57. https://doi.org/10.1016/j.brainres.2009.06.081.

Uran, S.L., Caceres, L.G., Guelman, L.R., 2010. Effects of loud noise on hippocampal and cerebellar-related behaviors. Role of oxidative state. Brain Res. 1361, 102–114. https://doi.org/10.1016/j.brainres.2010.09.022.

Wakabayashi, K., Fujioka, M., Kanzaki, S., Okano, H.J., Shibata, S., Yamashita, D., Masuda, M., Mihara, M., Ohsugi, Y., Ogawa, K., Okano, H., 2010. Blockade of interleukin-6 signaling suppressed cochlear inflammatory response and improved hearing impairment in noise-damaged mice cochlea. Neurosci. Res. 66, 345–352. https://doi.org/10.1016/j.neures.2009.12.008.

Wang, S., Wang, Y.-J., Su, Y., Zhou, W., Yang, S., Zhang, R., Zhao, M., Li, Y., Zhang, Z., Zhan, D., Liu, R., 2012. Rutin inhibits β-amyloid aggregation and cytotoxicity, attenuates oxidative stress, and decreases the production of nitric oxide and proinflammatory cytokines. Neurotoxicology 33, 482–490. https://doi.org/10.1016/j.neuro.2012.03.003.

Whitehead, K.J., Smith, C.G.S., Delaney, S.-A., Curnow, S.J., Salmon, M., Hughes, J.P., Chessell, I.P., 2010. Dynamic regulation of spinal pro-inflammatory cytokine release in the rat in vivo following peripheral nerve injury. Brain Behav. Immun. 24, 569–576. https://doi.org/10.1016/j.bbi.2009.12.007.

Wohleb, E.S., Patterson, J.M., Sharma, V., Quan, N., Godbout, J.P., Sheridan, J.F., 2014. Knockdown of interleukin-1 receptor type-1 on endothelial cells attenuated stress-induced neuroinflammation and prevented anxiety-like behavior. J. Neurosci. 34, 2583–2591. https://doi.org/10.1523/JNEUROSCI.3723-13.2014.

Yan, S.D., Chen, X., Fu, J., Chen, M., Zhu, H., Roher, A., Slattery, T., Zhao, L., Nagashima, M., Morser, J., Migheli, A., Nawroth, P., Stern, D., Schmidt, A.M., 1996. RAGE and amyloid-beta peptide neurotoxicity in Alzheimer's disease. Nature 382, 685–691. https://doi.org/10.1038/382685a0.